Title

Synergistic effect of nanodiamonds on the adsorption of tricresyl phosphate on iron oxide surfaces

Journal

Applied Physics Letters, 114(17)

ISSN

0003-6951

Authors

Khajeh, Arash
Krim, Jacqueline
Martini, Ashlie

Publication Date

2019-04-29

DOI

10.1063/1.5093425

Peer reviewed

Cite as: Appl. Phys. Lett. 114, 171602 (2019); https: //doi.org/10.1063/1.5093425

Synergistic effect of nanodiamonds on the adsorption of tri-cresyl phosphate on iron oxide surfaces

Arash Khajeh and Ashlie Martini*
Department of Mechanical Engineering, University of California Merced, 5200 N. Lake Rd, Merced, CA 95343, USA

Jacqueline Krim
Department of Physics, North Carolina State University, 2401 Stinson Dr, Raleigh, NC 27607, USA

ABSTRACT

Nanodiamonds (NDs) have potential uses in many applications, including as additives for liquid lubricants, where they may be combined with more traditional chemicals to form protective films on sliding surfaces. It has been shown that NDs can function synergystically with tri-cresyl phosphate (TCP) to facilitate film formation on air baked iron. Here, reactive molecular dynamics simulations of TCP and NDs on an amorphous iron oxide surface reproduce experimental observations of the temperature at which film formation begins with NDs present and the effect of NDs on film composition. Analysis of chemical bonding in the simulations shows that the film formed in the presence of NDs is comprised of NDs and TCP that are both directly and indirectly bonded to the surface. Notably, the amount of phosphorous in the film, which is important for surface protection, is increased by TCP molecules that are indirectly bonded to the surface via NDs, which suggests that indirect bonding is one mechanism by which NDs facilitate film growth. The synergy of NDs and TCP has important implications for the development of NDs as emerging lubricant additives which must function with existing additives such as TCP in many applications.

I. INTRODUCTION

Chemical reactions between liquid phase species and a solid surface are the precursors to growth of solid or semi-solid films in a variety of applications. Understanding the pathways for these reactions is therefore an important step towards optimization of film growth parameters [1, 2]. Here, we focus on reactions between tri-cresyl phosphate (TCP) and an amorphous iron oxide surface. This is an important system because TCP is a chemical additive that is included in lubricant formulations to minimize wear of moving components. TCP is widely used in lubricants in the aviation industry as well as some automotive engines [3]. In a mechanical system, TCP functions by chemically reacting with ferrous surfaces to form films that protect those surfaces from wear under harsh sliding conditions [4, 5].

Despite the success of TCP as a lubricant additive, it is associated with environment and health concerns that encourage the development of alternatives [6, 7]. However, emerging lubricant additives must, at least initially, be compatible with existing additives such as TCP. One family of emerging lubricant additives that has been the focus of many studies in recent years is nanoparticles [8]. Of particular interest for some applications are diamond nanoparticles, or nanodiamonds (NDs), which offer high thermal conductivity, high hardness, high melting point and the ability to withstand extreme environments [9]. ND additives have been shown to reduce friction and wear in both oil- and water-based lubricated systems [9–14]. However, the compatibility of NDs with existing lubricant additives, including TCP, is not yet fully understood.

Of particular concern is the fact that NDs have been reported to increase the activation energy for some processes [15], which could adversely affect TCP–surface reactions and in turn limit TCP film growth. However, recently, a quartz crystal microbalance (QCM) was used as an *in situ* tool [16] to measure reaction temperatures of TCP on ferrous surfaces [17]. These measurements showed that, contrary to expectation, the addition of NDs facilitated the formation of TCP films on air baked Fe surfaces [18]. The composition of the resultant film was also found to be affected by the NDs, with the presence of NDs increasing the amount of carbon and oxygen relative to the amount of iron in the film. These findings were extremely promising because they showed that NDs can have a synergistic effect on the formation of protective films in lubricated contacts [18]. However, the experimental approach did not provide a fundamental explanation for the observed benefit of NDs on TCP films. Therefore, here we use molecular dynamics simulations (MD) here to explore the interactions between TCP, NDs and amorphous iron oxide surfaces to explain the underlying physics.

II. METHODS

Simulations were designed to capture chemical reactions between TCP molecules and an amorphous iron oxide surface, with and without NDs, across the same range of temperatures reported in the previous QCM study. Two models were created, one with NDs and one without NDs, as shown in Fig. 1. In both systems, the dimensions of simulation domain were 5 nm $\times$ 5 nm $\times$ 10 nm, with periodic boundaries in the plane of the surface and a fixed boundary in the surface–normal direction. A repulsive wall at the height of 9.8 nm was employed to prevent atoms from traveling out of the simulation box. Both models contained 32 TCP molecules, corresponding to approximately a monolayer, and one of the systems also con-

* amartini@ucmerced.edu

tained 5 NDs. All interactions were described by the ReaxFF force field [19], which enabled the model to capture formation and breaking of covalent bonds, with a recently developed parameter set that captured all relevant atomic interactions [20]. In both systems, atoms in the bottom 0.3 nm of the iron oxide were fixed in place. Temperature was controlled using a Nosé-Hoover thermostat with a damping parameter of 25 fs applied to all unconstrained atoms. Simulations were run using LAMMPS [21] with a time step of 0.25 fs.

The amorphous iron oxide was created by annealing a slab of crystalline Fe_2O_3 iron oxide (5 nm $\times$ 5 nm in the plane of the surface and 1.7 nm thick). Annealing was performed by increasing the temperature from 300 to 4000 K over 25 ps, holding at 4000 K for 125 ps, and then decreasing back to 300 K over 500 ps [20]. The surface was then passivated by introducing water molecules into the model. A simulation with the amorphous iron oxide surface and water was run at 700 K for 500 ps, after which the number of chemical bonds was constant. After the simulation, any water molecules not covalently bonded to the surface were removed from the model. The hydroxyl group density on the final surface was 8.31 nm^{-2}, consistent with the range of 5 to 9 nm^{-2} reported in previous studies [22]. The resultant passivated amorphous iron oxide model was comparable to the surface of the sample used in previous experimental measurements of a pure iron film baked in air at 513 K for two hours [18].

The ND particles were created by cutting from a block of carbon atoms in a diamond structure such that the surfaces of the cut material had the minimum energy [23]. The resultant particles had a diameter of approximately 1 nm. The NDs were passivated by placing them in a simulation with water molecules at 500 K for 500 ps. During the hydroxylation process, water molecules reacted with the ND surface leading to the formation of CH and COH chemical groups. The observation of hydrogen and hydroxyl terminated carbon atoms on the surface of NDs has been reported in previous studies [24]. In the QCM experiments, the NDs had a diameter of 30 nm and, in an oil dispersion, were prepared in a manner that is expected to result in COOH termination. The presence of COOH groups is expected based on previous experimental observations [25] as this chemistry has been shown to improve dispersion by promoting electrostatic attraction with the anchoring groups of the dispersants [10]. Thus, our model NDs were several times smaller than those in the experiment and likely had different termination. The size scale was limited by the simulation method and the termination was determined by the force field through the simulation of the NDs with water. Despite these differences, the model NDs were a reasonable approximation since all of the reactions that we observed were between the un-terminated C atoms in the NDs and either O from the TCP or Fe on the surface.

Both models were initially equilibrated at room temperature for 0.25 ns. Then, the temperature was increased linearly at a rate of 1000 K/ns to a maximum temperature of 550 K. This is the same temperature range as reported in the previous QCM experiments [18], although the heating rate was orders of magnitude faster than in the experiments due to the small time scale of the model. The simulation was repeated three times for each model to enable statistical analysis of results. For each replica, the TCP molecules were placed at different initial positions such that the simulations captured the potential interaction of TCP with many different reactive sites on the surface. Also, to confirm the heating rate did not affect results, simulations were repeated once more at a rate of 500 K/ns. During the simulation, the number and type of covalent bonds between TCP and the iron oxide surface were recorded.

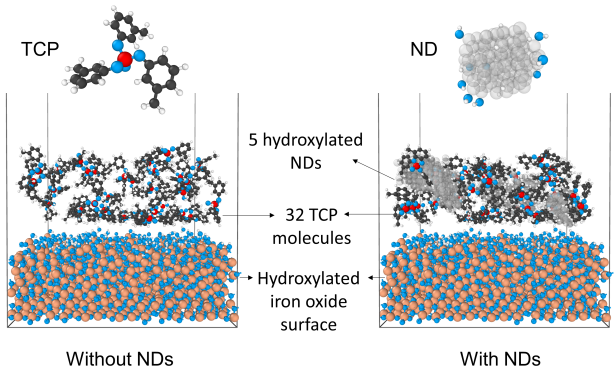

FIG. 1. Snapshots of the simulations consisting of TCP molecules on an amorphous iron oxide surface, with and without NDs. Close-up views of the TCP and ND are shown as insets above the simulation snapshots. Colors represent: Hydrogen - white, Oxygen - blue, Phosphorous - red, carbon in TCP - black, carbon in NDs - faded grey.

III. RESULTS AND DISCUSSION

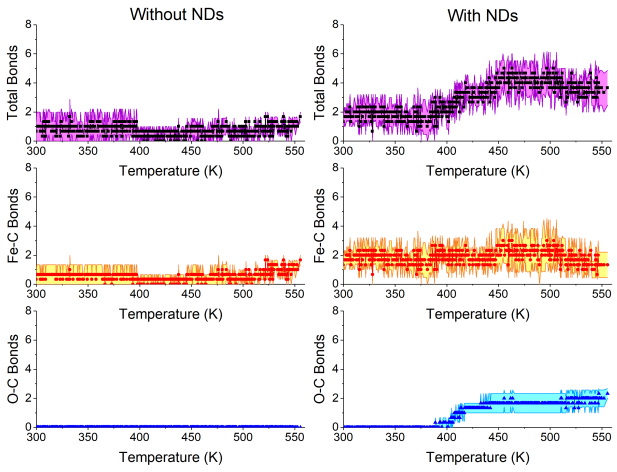

FIG. 2. Number of covalent bonds formed between TCP and the iron oxide surface as a function of temperature without (left) and with (right) NDs as a function of temperature. The top figures show the total number of bonds and the middle and bottom figures show the number of Fe–C and O–C bonds, respectively. The symbols are the average and the lines/shading represent the standard error of the three independent simulations.

Figure 2 shows the number of bonds between TCP molecules and the iron oxide surface, with and without NDs present. At all temperatures, the chemical bonds that formed were between C atoms in the TCP and either Fe or O atoms on the surface. Two key observations can be made from these results. First, there were more chemical bonds formed between TCP and the surface when the NDs were present. This is consistent with the observation from QCM experiments on air baked Fe which showed an abrupt frequency shift (indicating film growth) only for the system with NDs [18]. Second, the increase in bonding with NDs observed in Fig. 2 occurred between 400 and 470 K. This is similar to the temperature of the abrupt frequency shift in the QCM experiments which occurred at 500 K [18]. Further, the frequency shift observed at a single temperature on the experimental time scale is captured by the orders-of-magnitude faster simulations as an increase in bonding over a range of temperatures, potentially explaining why the shift is so abrupt in the experiments. These same trends were observed in our simulations at the slower temperature ramp rate of 500 K/ns.

To better understand the elementary steps leading to TCP film formation in the presence of NDs, we analyzed individual chemical bonds formed during the simulation. The unique bonding sites on the TCP are differentiated and identified in the upper panel of Fig. 3. We observed that most of the direct TCP–surface bonds were formed between the C5 or the C6 of the TCP and Fe on the surface. Representative snapshots of these bonds are shown in the middle panel of Fig. 3. We also observed direct chemical bonding between the ND and the surface via Fe–C_{ND} bonds. This is consistent with experimental detection of NDs embedded in the film grown in QCM as shown in the insets to Fig. 4. Finally, the simulations showed bonding between C atoms in the NDs and the double-bonded O atom in the TCP. In many cases the NDs to which the TCP molecules bonded were themselves bonded to the surface. Therefore, the NDs provide a means of indirectly bonding the TCP to the surface. This observation suggests that the NDs contribute to film formation by enabling indirect bonding between the TCP and surface.

We next analyzed the composition of the film forming on the surface through these reactions at 490 K, a temperature near which bonding was observed in the simulations and the frequency shift was measured in the experiments. From the simulations, we calculated the surface density of each type of atom that was either directly or indirectly bonded to the surface. An example of an indirectly bonded atom is an atom in a TCP molecule chemically bonded to an ND that is chemically bonded to the surface. Figure 4 shows that the densities of all atom types (C, O and P) were dramatically larger in the system with NDs. These results are consistent with the film composition reported from the experimental study obtained using electron dispersive X-ray spectroscopy (EDS) [18]. In the experiments, the molar composition of the film without NDs was 9.8 for C, 7.6 for O and 0.02 for P; with the NDs it was 20.0 for C, 18.0 for O and 0.3 for P. The same trend is observed in Fig. 4 where the density of all elements is greater with the NDs present, and the relative amount of each element increases as P<O<C both with and without NDs. The ratio of

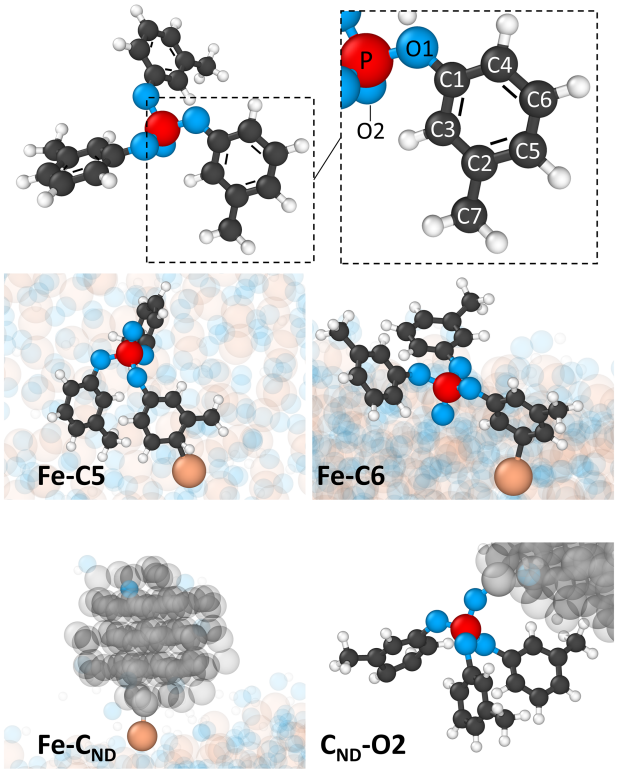

FIG. 3. Snapshots from simulations illustrating the most commonly observed reactions between TCP, the iron oxide surface and the NDs. All atoms are faded except those involved in a given reaction. The unique reaction sites on the TCP are labeled in the upper panel.

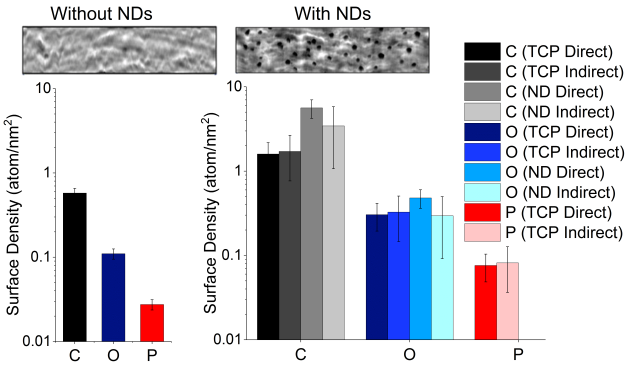

FIG. 4. Simulation surface density of carbon, oxygen and phosphorous in the film at 490 K, quantified by the number of atoms in the TCP or NDs that are directly or indirectly bonded to the surface. Inset are 300 nm × 1500 nm atomic force microscope topography images (height scale is approximately 36 nm dark to light) of the film grown in QCM experiments; adapted from the graphical abstract of Ref. [18].

C to O is higher in experiments than in simulations, which is attributable to the fact that the experimental measurement captured both the film and substrate on which it formed, while the simulation calculation included only atoms from the TCP and

NDs. The compositions of all three elements increased in the presence of the NDs, both in experiments and simulations. In the simulations, it was found that that the increase was due to both NDs directly bonded to the surface, as well as TCP molecules and NDs indirectly bonded to the surface (Fig. 4). This effect is particularly relevant for P, which is an important constituent of the film in terms of reducing wear in moving components. Here, we show that indirectly bonded TCP molecules contribute significantly to the increased amount of P in the film with NDs. These results suggest that one mechanism by which the NDs facilitate film formation is the ability to indirectly bond the TCP to the surface.

IV. CONCLUSIONS

In summary, we used reactive molecular dynamics simulation to investigate the origins of previously observed differences between TCP film formation on ferrous surfaces with and without NDs present. First, the simulations showed that NDs increased the number of bonds between TCP and iron oxide – this is consistent with the measurement of a frequency shift at 500 K in QCM experiments with NDs, indicating film formation. Second, analysis of individual chemical bonds in the simulation showed that TCP can bond with the surface both directly and indirectly. The direct bonding was shown to occur primarily between the C5 and C6 on the TCP and Fe on the surface. The indirect bonding of TCP molecules was shown to occur through the O atom on the TCP bonding with C on the ND, where that ND was bonded to the surface. Next, simulation results revealed a higher density of C, O and P directly or indirectly bonded to the surface in the presence of NDs, comparable to EDS measurements of a higher percent of those elements with NDs. The higher density of elements originally from the TCP is in part due to TCP molecules bonded to the surface via an ND. These finding reveal that the NDs can facilitate film formation through their ability to bond TCP molecules indirectly to the surface. The simulations thus support and then explain the previous experimental findings of synergy between NDs and TCP. Taken together, the experiments and simulations show that, contrary to expectations, NDs do not suppress TCP–surface reactions, which encourages use of these additives in lubricated components.

Acknowledgements
The authors thank Dr. Stephen Berkebile for discussion and helpful feedback on this project. AM and AK acknowledge support from the Army Research Laboratory under Cooperative Agreement Number W911NF-16-2-0121. JK acknowledges support from the National Science Foundation through grant DMR-1535082 as well as O. Shenderova and B. Acharya for useful discussions.

[1] A. L. Lloyd, Y. Zhou, M. Yu, C. Scott, R. Smith, and S. D. Kenny. Reaction pathways in atomistic models of thin film growth. *J. Chem. Phys.*, 147:152719, 2017.

[2] K. Mohammadtabar, S. J. Eder, P. O. Bedolla, N Dörr, and A. Martini. Reactive molecular dynamics simulations of thermal film growth from di-tert-butyl disulfide on an fe(100) surface. *Langmuir*, 34:15681–15688, 2018.

[3] D. Johnson and J. Hils. Phosphate esters, thiophosphate esters and metal thiophosphates as lubricant additives. *Lubricants*, 1:132–148, 2013.

[4] B. Guan, B. A. Pochopien, and D. S. Wright. The chemistry, mechanism and function of tricresyl phosphate (TCP) as an anti-wear lubricant additive. *Lubrication Sci.*, 28(5):257–265, 2016.

[5] E. Osei-Agyemang, S. Berkebile, and A. Martini. Decomposition mechanisms of anti-wear lubricant additive tricresyl phosphate on iron surfaces using dft and atomistic thermodynamic studies. *Tribol. Lett.*, 66(1):48, 2018.

[6] S. Michaelis. Contaminated aircraft cabin air. *J. Biol. Phys. Chem.*, 11:132–145, 2011.

[7] J.J. Ramsden. On the proportion of ortho isomers in the tricresyl phosphates contained in jet oil. *J. Biol. Phys. Chem.*, 13:69–72, 2013.

[8] W. Dai, B. Kheireddin, H. Gao, and H. Liang. Roles of nanoparticles in oil lubrication. *Tribol. Int.*, 102:88–98, 2016.

[9] A. Raina and A. Anand. Tribological investigation of diamond nanoparticles for steel/steel contacts in boundary lubrication regime. *Appl. Nanosci.*, 7:371–388, 2017.

[10] M. Ivanov and O. Shenderova. Nanodiamond-based nanolubricants for motor oils. *Curr. Opin. Solid St. M.*, 21(1):17–24, 2017.

[11] I. Ali, A. Kucherova, N. Memetov, T. Pasko, K. Ovchinnikov, V. Pershin, D. Kuznetsov, E. Galunin, V. Grachev, and A. Tkachev. Advances in carbon nanomaterials as lubricants modifiers. *J. Mol. Liq.*, 279:251–266, 2019.

[12] N. Nunn, Z. Mahbooba, M.G. Ivanov, D.M. Ivanov, D.W. Brenner, and O. Shenderova. Tribological properties of polyalphaolefin oil modified with nanocarbon additives. *Diam. Relate. Mater.*, 54:97–102, 2015.

[13] A. Shirani, N Nunn, O. Shenderova, E. Osawa, and D. Berman. Nanodiamonds for improving lubrication of titanium surfaces in simulated body fluid. *Carbon*, 143:890–896, 2019.

[14] Y. Jiao, S. Liu, Y. Sun, W. Yue, and H. Zhang. Bioinspired surface functionalization of nanodiamonds for enhanced lubrication. *Langmuir*, 34:12436–12444, 2018.

[15] Y. Tong, R. Liu, and T. Zhang. The effect of a detonation nanodiamond coating on the thermal decomposition properties of rdx explosives. *Phys. Chem. Chem. Phys.*, 16:17648–17657, 2014.

[16] B. Acharya, M. A. Sidheswaran, R. Yungk, and Krim J. Quartz crystal microbalance apparatus for study of viscous liquids at high temperatures. *Rev. Sci. Inst.*, 88:025112, 2017.

[17] B. Acharya, T. N. Pardue, K. S. Avva, and Krim J. In situ, real time studies of thermal reaction film formation temperatures for iron and 304ss surfaces immersed in 5% tricresyl phosphate in base oil. *Tribol. Int.*, 126:106–115, 2018.

[18] B. Acharya, K. Avva, B. Thapa, T. Pardue, and J. Krim. Synergistic effect of nanodiamond and phosphate ester anti-wear additive blends. *Lubricants*, 6(2):56, 2018.

[19] A. C. T. van Duin, S. Dasgupta, F. Lorant, and W. A. Goddard. ReaxFF: A reactive force field for hydrocarbons. *Phys. Chem. A*, 105:9396–9409, 2001.

[20] A. Khajeh, X. Hu, K. Mohammadtabar, Y. K. Shin, A. van Duin, S. Berkebile, and A. Martini. Statistical analysis of tricresyl phosphate conversion on an iron oxide surface using reactive molecular dynamics simulations. *J. Phys. Chem. C*, submitted, 2019.

[21] S. Plimpton. Fast parallel algorithms for short-range molecular dynamics. *J Comp Phys*, 117:1–19, 1995.

[22] J. P. Hsu. *Interfacial forces and fields: Theory and applications*, volume 85. CRC Press Inc., Boca Raton, Florida, 1999.

[23] G. Kern and J. Hafner. Ab initio calculations of the atomic and electronic structure of clean and hydrogenated diamond (110) surfaces. *Phys. Rev. B*, 56:4203, 1997.

[24] D. Ho. *Nanodiamonds: applications in biology and nanoscale medicine*. Springer Science & Business Media, 2009.

[25] O. A. Williams. *Nanodiamond*. Royal Society of Chemistry, 2014.